Experimental Study on Digital Image Correlation for Deep Learning-Based Damage Diagnostic

Nur Sila Gulgec * Martin Takáč † Shamim N. Pakzad ‡

Abstract

Large quantities of data which contain detailed condition information over an extended period of time should be utilized to prioritize structures and infrastructure repairs. As the temporal and spatial resolution of monitoring data drastically increases by advances in sensing technology, structural health monitoring applications reach the thresholds of big data. Deep neural networks are ideally suited to use large representative training datasets to learn complex damage features. In the previous study of authors, a real-time deep learning platform was developed to solve damage detection and localization challenge. The network was trained by using simulated structural connection mimicking the real test object with a variety of loading cases, damage scenarios, and measurement noise levels for successful and robust diagnosis of damage. In this study, the proposed damage diagnosis platform is validated by using temporally and spatially dense data collected by Digital Image Correlation (DIC) from the specimen. Laboratory testing of the specimen with induced damage condition is performed to evaluate the performance and efficiency of damage detection and localization approach.

Keywords Structural health monitoring • Digital Image Correlation • Convolutional Neural Networks • Damage Detection

1 Introduction

It is important to establish lifetime safety of the infrastructure subjected to a wide range of environmental and operational conditions [1]. Providing timely damage assessment of these structures often requires long-term monitoring and dense instrumentation techniques [2]. Sensor networks today provide an exciting set of opportunities and challenges to collect an enormous amount of data from any structure, which due to its nature is posing a big data problem [3]. Conventional approaches primarily focus on hand-crafting damage features and classifiers to interpret the health condition of the structures [4, 5, 6, 7]. Although such methods are effective in identifying structural damage of a particular type, there are some constraints limiting these methods. The existing methods of analysis rely on estimating carefully crafted features that often are limited in what they can do and are not automated in nature, thus not appropriate for a broad range of big data applications [8, 9].

Deep Neural Networks (deep learning or DNN) is a state-of-the-art set of methods for taking advantage of the opportunities hidden in big data. They are designed such that they can learn from data, for this reason, deep learning is ideally suited to use large representative training datasets to learn complex features [10]. DNNs learn by training which is then used to make data-driven predictions or decisions. One of the most widely used types of DNN is convolutional neural network (CNN) due to its ability to keep spatial features of the input and reduce memory requirements by using fewer parameters [11, 12].

The prior studies of authors [13, 14] addressed these issues by developing a CNN-based real-time for damage identification and localization methodology that learns sophisticated data-driven damage features without extracting hand-designed damage features. The approach fed the network by using raw strain field measurements which are a direct indicator of stress, fatigue, and failure. The algorithm was trained and validated successfully on test cases created by FE simulations.

In this paper, the performance of the trained algorithm is tested by using data collected by an optic-based technique called digital image correlation (DIC)[15]. Full-field measurement data obtained by DIC helps to understand the local effects and

*Ph.D. Candidate, Department of Civil and Environmental Engineering, Lehigh University, 117 ATLSS Drive, Imbt Labs, Bethlehem, PA 18015, USA.

†Assistant Professor, Department of Industrial and Systems Engineering, Lehigh University, 200 West Packer Avenue, Harold S. Mohler Laboratory, Bethlehem, PA 18015, USA.

‡Associate Professor, Department of Civil and Environmental Engineering, Lehigh University, 117 ATLSS Drive, Imbt Labs, Bethlehem, PA 18015, USA.

material and component behavior. In this study, the feasibility of the CNN-based method is evaluated by using the data collected by DIC.

The rest of the paper is organized as follows. First, a brief explanation of the CNN-based methodology is provided in Section 2; then, the test setup is described in Section 3. In Section 4, experimental validation of the proposed CNN architecture and the main findings are presented. Conclusions and future directions are given in Section 5.

2 CNN-Based Approach for Robust Structural Damage Diagnosis

In this section, the adopted technique [13] is briefly described. As presented in Figure 1, a general map of the algorithm is composed of a training and testing phase. Training phase operates on the strain fields obtained from finite element simulations. After normalizing each strain field by its absolute maximum, the search mechanism finds a good set of hyperparameters. Once the network architecture is built by these hyperparameters, it is trained to determine the existence of damage (i.e. detection task) and estimate the boundaries of the damaged area (i.e. localization task). Both of the tasks share trainable parameters to extract local features which are common for them. This provides more efficient learning, shorter training time and lower computation cost. Trained parameters are saved to test the performance of strain field collected by DIC system. In this phase, raw strain fields are fed into the proposed architecture to estimate the labels for detection and localization tasks.

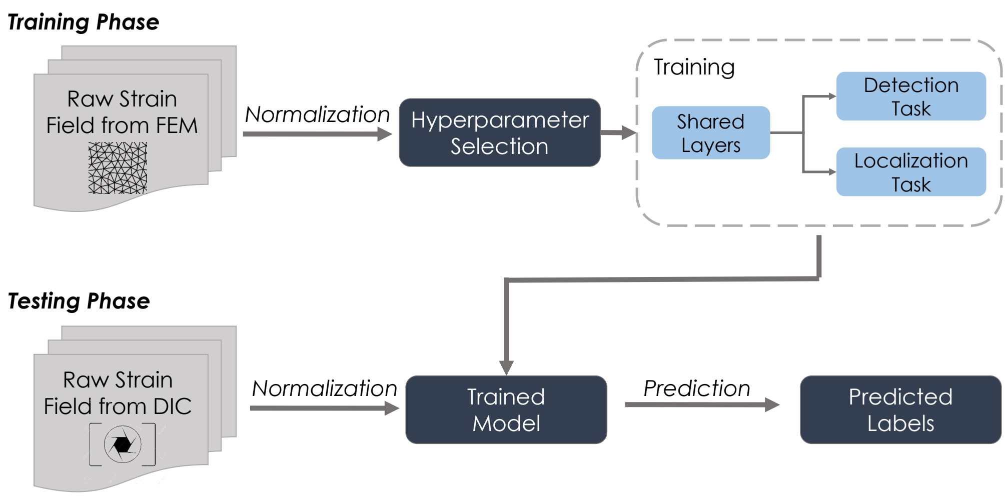

Figure 1: Overview of the proposed methodology.

Training data is formed by using FE simulations of a connection shown in Figure 3a. The connection consists of two 20 inch-long C8x11.5 channels welded to a steel plate with the dimension of 28x14x1/4 inches. Each channel member has 8-inch overlap with the main gusset plate. The material is considered as elastic-perfectly plastic with a yield strength of 36 ksi. A total of 30,000 healthy and 30,000 damaged samples are generated with different loads, damage locations and measurement noise. Damage is modeled as 0.5 inch long cracks where coordinates are randomly selected from the area bounded by the two corners $[A(8.5, 1)$ and $B(19.5, 13])$. The crack coordinates which are used to create training dataset are shown as black lines in the Figure 3a. The location of the crack is stored as bounding box (a_1, b_1, a_2, b_2), where b_1 and b_2 indicate the coordinates of the tips of the crack; a_1 and a_2 are the y coordinate of the crack with 0.5 inch subtraction and addition, respectively. For the "healthy" samples, bounding box is set to $[0, 0, 0, 0]$.

Varying loads between $\sim U$[-100 kips (compression), 120 kips (tension)] are applied to the end of the channels. Additive Gaussian noise $\sim N(0, \sigma^2)$ is added to noise-free samples where σ is the standard deviation of the measurement noise. Four different noise levels (i.e. the ratio between the standard deviation of measurement noise to actual strain values) is considered (2%, 5%, 10%, and 15%). Strain distribution in the direction of loading (ε_y) is represented as 28x56x1 tensors, then utilized to feed the CNN architecture.

The network found by hyperparameter search mechanism is shown in Figure 2. It consists of three convolutional layers followed by two task-specific fully connected layers. The convolutional layers receive the input layer and pass them through a filter size of $(3\text{x}3)$. The network forms 8, 16 and 32 feature maps after these convolutional layers. The max-pooling operation, which has the size of $(2\text{x}2)$ with a stride of 2, performs right after first and second convolution layer. The feature maps of the last convolutional layer are stacked together in an array and employed as an input to the task-specific layers. The hidden layer sizes for the detection task are $[836-767]$, whereas they are $[1305-1191-406]$ for the localization task. The learning rate of $\eta_{det}=0.0451$ and $\eta_{loc}=0.0026$ are adopted for the detection and localization parts, respectively.

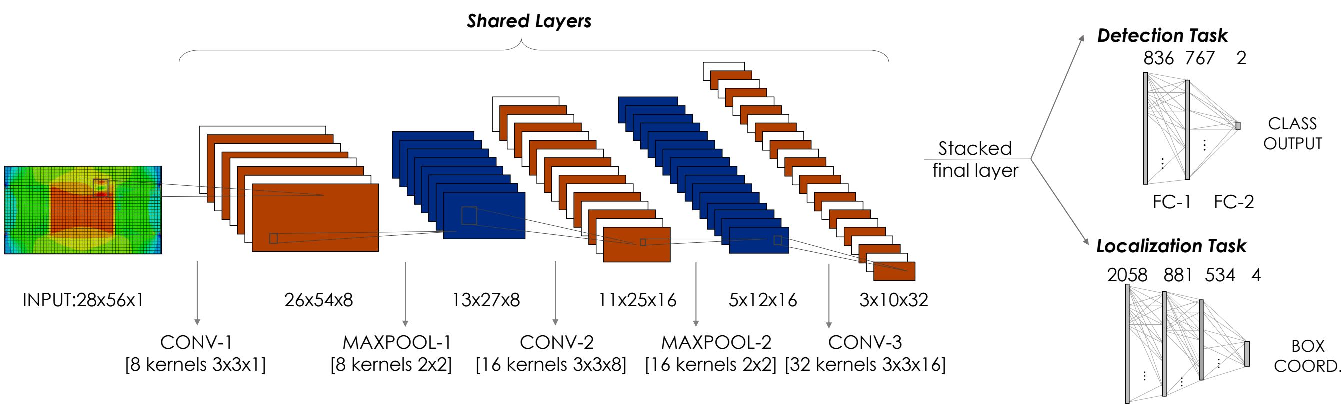

Figure 2: Proposed CNN architecture.

3 Experimental Validation

3.1 Test Setup

The principal behind DIC methodology is to determine the shift and/or rotation of elements of a reference image in an image taken under different conditions [16]. Figure 3 illustrates the test setup including the specimen, GOM Aramis 3D DIC system, and external light sources. A structural connection includes a stochastic pattern on the front surface of the specimen to track the changes in the gray-scale. In order to create the pattern, white paint is sprayed to generate the background, then black speckles are randomly spread with a rubber stamp. The closer look to the pattern is presented in Figure 3b. The average speckle size of $1/8$ inch is obtained. Damage is created as a grinded dent through the thickness from the coordinate (9, 17.5) to (10, 17.5) inches which was not used in the training dataset (Figure 3a).

3D DIC system includes two high resolution (4000 x 3000 pixels) cameras with high precision lenses with a focal length of 24 mm. The cameras position 35 inches away from the specimen with 14.4-inch distance between the cameras to capture approximately 14x20 inch measurement volume. Polarize filters are attached to the lenses to remove glare and get consistent illumination. Calibration is done with coded panels to achieve good accuracy in both in-plane and out-of-plane measurements. The external light source is utilized to illuminate the specimen and balance the effect of the ambient light existing in the laboratory.

Dense strain measurements of the specimen are collected during different stages of the damage. The test is conducted within the linear elastic range of the material behavior. The plate is gradually loaded to 50 kips and unloaded to its zero-load position by using the SATEC 600kip hydraulic testing system. The quasi-static loading scheme is presented in Figure 3c. In every 5 kip load increment, the load is held for a minute to allow DIC to take pictures. For each constant load, 150 pictures are acquired with the sampling rate of 4 Hz.

3.2 Analysis of Data

ARAMIS Professional 2017 software [17] is used to achieve full-field analysis of the test object. The software evaluates high-resolution images recorded from the specimen during loading, then automatically computes 3D coordinates for all loading stages and derives strain results. The post-processing algorithm of software has a stage-wise analysis, in which each stage consists of one image. In this study,the reference image is selected as the first image taken under the load of 5 kips. Then, axial strain fields (ε_y) are computed as an input to trained network architecture. An example of strain field stages from each ten load levels {5 kip, 10 kip, ..., 50 kip} is shown in Figure 4. The axis of the colorbar is set to $[-200, 1000]$ μm/m for all stages to illustrate the effect of the crack on the axial strain. The histogram of the strain values is also shown next to the legend. It is noticeable that strain gradients start to occur near crack tips when the load is greater than 35 kips.

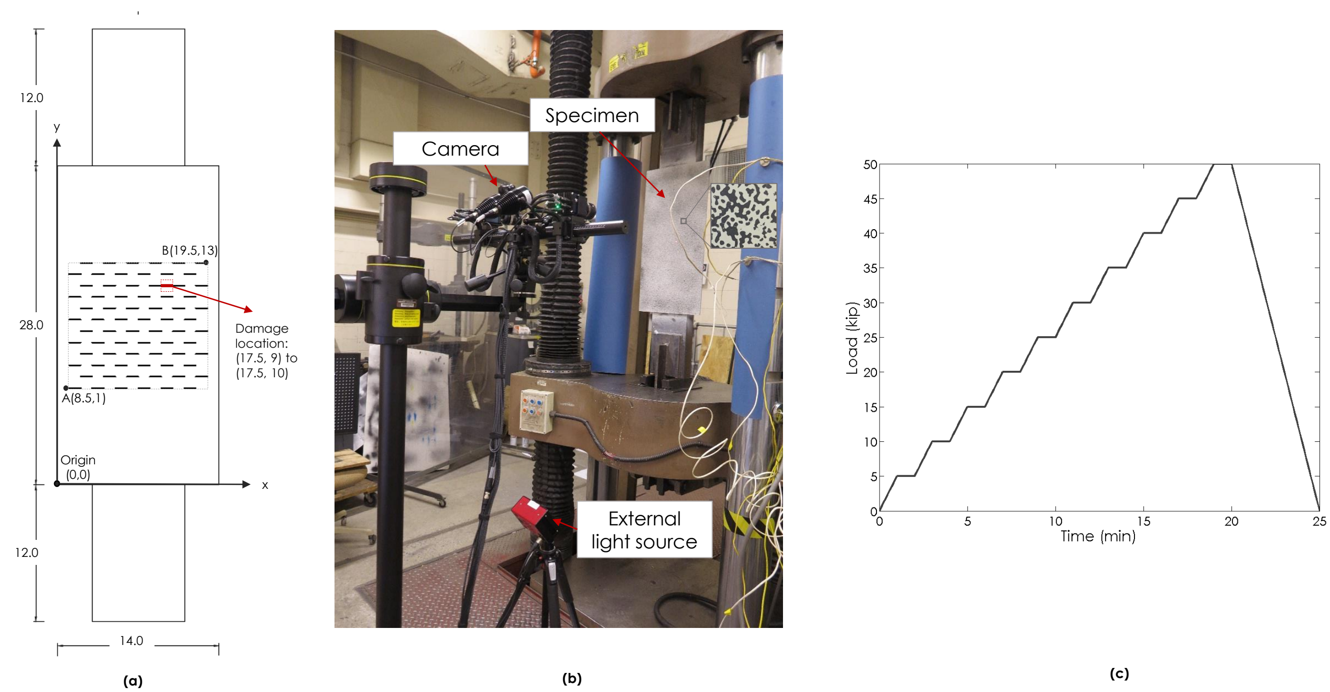

Figure 3: (a) Specimen, (b) Test setup, (c) Loading scheme.

In order to better analyze the measurements, the strain measurement obtained from several cross sections (i.e. Plane Y = 12.5, 13, 15.5 inches) are plotted for all load stages (Figure 5). In the figure, each line represents 150 stages that have been averaged together and each color indicates the strain measurements at a specific load. The figure shows that strains increase linearly in a similar trend with each consecutive loading. In other words, the difference of the measurements at 50 kips and 45 kips are identical with the measurements at 45 kips and 40 kips. The only exception is observed for loads smaller than 15 kips where the maximum strain is less than $100\ \mu m/m$. This level of strain measurement is accepted as noise floor which is very difficult to measure for the size of the specimen.

4 Damage Detection and Localization Results

This section evaluates the performance of the trained network on data collected from DIC for detection and localization tasks. The data is sampled from every 0.5 inch to adapt the mesh size in FE model. Since cameras capture 14x20 inch measurement volume, the areas that are not covered by the cameras are filled by padding zeros. In the end, strain fields of 28x56x1 tensors are normalized by its absolute maximum are tested by saved model parameters. Detection accuracy is defined as the correct prediction of a sample being damaged or healthy. Detection performance of the network is visualized in Figure 6a. All samples from different loading stages are correctly identified. It is worthwhile to mention that high detection accuracy is accomplished although there were strain gradients caused by other imperfections rather than the crack. High stress concentrations are also observable near the welds.

Further analysis is achieved by performing the localization task since the data from healthy samples are not available. In this task, the accuracy is defined as predicted values being within the boundaries pre-defined by the threshold values (i.e. for the threshold value of 0.5, bounding box expands from the sides of 0.5 inch). Three different thresholds are used such as thr = 0.5 inch, thr = 1 inch, thr = 2 inch. According to the Figure 6b, the proposed architecture localizes the crack with 100% accuracy when the threshold value is 0.5 inch and the load is greater than 30 kips. Although the accuracy seems to decrease for the small loads for thr = 0.5 inch, the accuracy reaches 80% when the crack location is searched in the larger area by increasing the threshold.

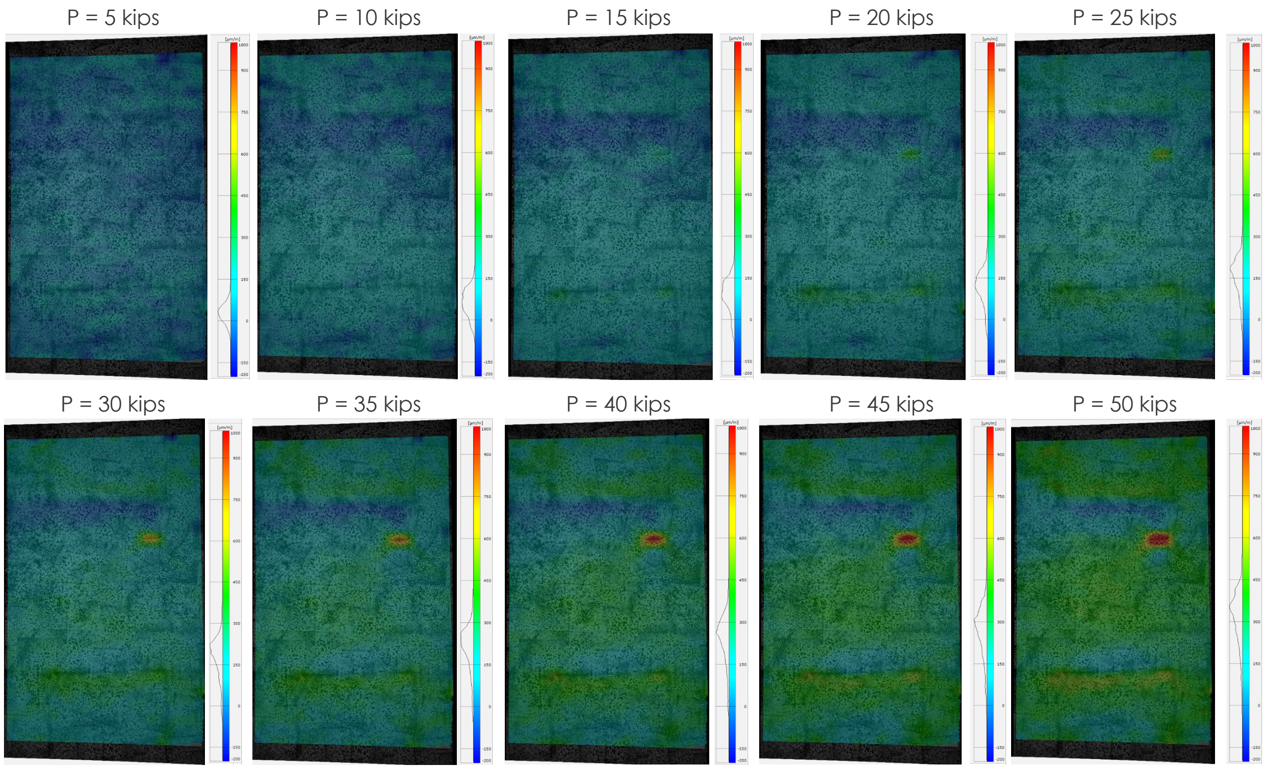

Figure 4: Strain fields.

5 Conclusion

In this study, the proposed real-time damage diagnosis platform is validated by using spatially dense data collected by Digital Image Correlation. Laboratory testing of the specimen with an induced damage condition is performed to evaluate the performance and efficiency of damage detection and localization approach.

Deep learning achieves remarkable generalization when it is designed carefully such that it can perform successfully even with unseen cases. In this study, designed architecture diagnoses damages on samples collected by DIC with high accuracy although training dataset only includes finite element simulations. Moreover, this generalization is observable for the localization task. The location of the crack was predicted successfully although the crack location was not given as input during training. Therefore, the proposed methodology is promising for automatizing the real-time structural damage diagnosis.

Acknowledgment. Research funding is partially provided by the National Science Foundation through Grant No. CMMI-1351537 by Hazard Mitigation and Structural Engineering program, and by a grant from the Commonwealth of Pennsylvania, Department of Community and Economic Development, through the Pennsylvania Infrastructure Technology Alliance (PITA). Martin Takáč was supported by National Science Foundation grant CCF-1618717 and CMMI-1663256.

References

[1] Hoon Sohn and Charles R Farrar. Damage diagnosis using time series analysis of vibration signals. *Smart materials and structures*, 10(3):446, 2001.

[2] X Fang, H Luo, and J Tang. Structural damage detection using neural network with learning rate improvement. *Computers & structures*, 83(25):2150–2161, 2005.

[3] Nur Sila Gulgec, Golnaz S Shahidi, Thomas J Matarazzo, and Shamim N Pakzad. Current challenges with bigdata analytics in structural health monitoring. In *Structural Health Monitoring & Damage Detection, Volume 7*, pages 79–84. Springer, 2017.

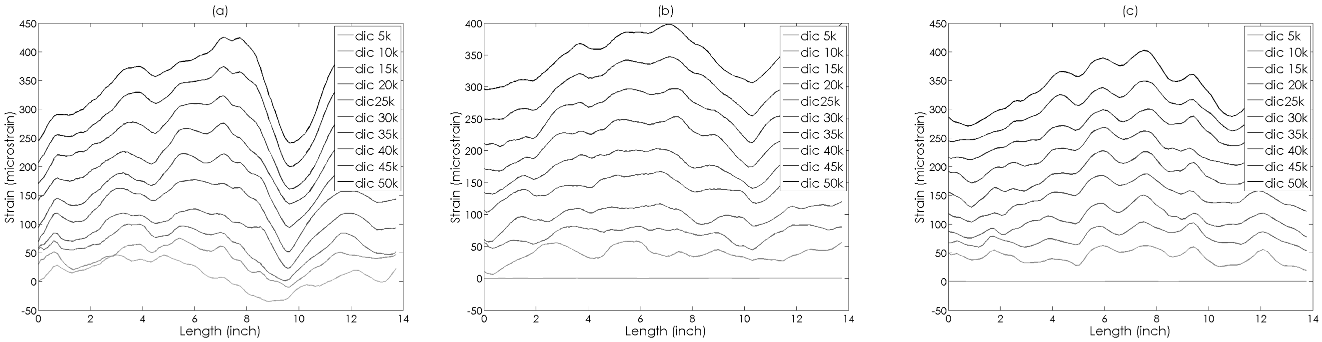

Figure 5: Strain values of the cross section at (a) Plane Y = 12.5 inch, (b) Plane Y = 13 inch, (c) Plane X = 15.5 inch.

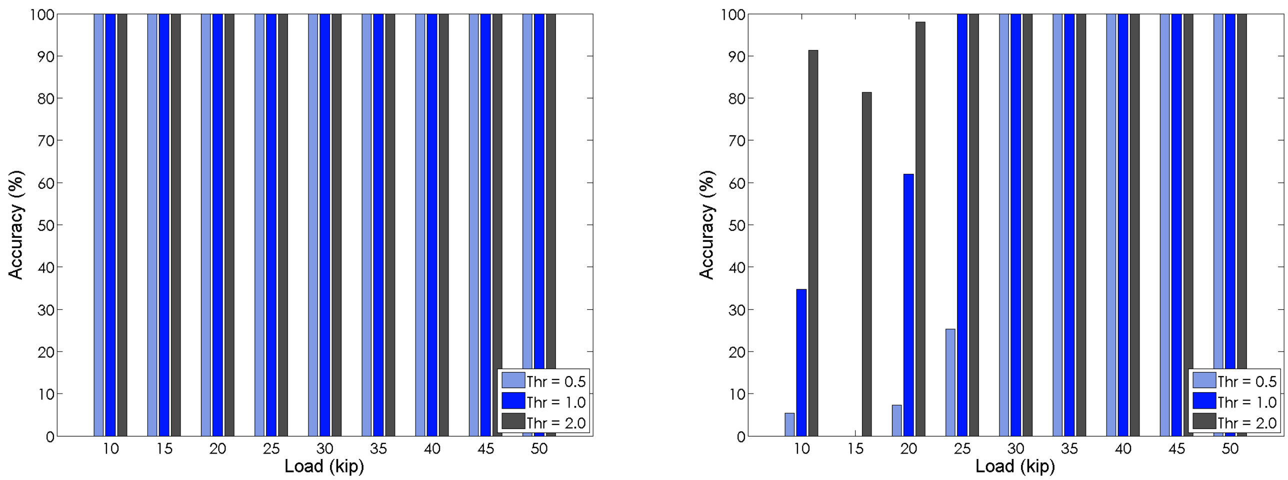

Figure 6: Performance of the network for (a) detection and (b) localization tasks.

[4] K Krishnan Nair, Anne S Kiremidjian, and Kincho H Law. Time series-based damage detection and localization algorithm with application to the asce benchmark structure. *Journal of Sound and Vibration*, 291(1):349–368, 2006.

[5] Ryohei Fujimaki, Takehisa Yairi, and Kazuo Machida. An approach to spacecraft anomaly detection problem using kernel feature space. In *Proceedings of the eleventh ACM SIGKDD international conference on Knowledge discovery in data mining*, pages 401–410. ACM, 2005.

[6] Arthur Shi and Xiao-Hua Yu. Structural damage detection using artificial neural networks and wavelet transform. In *2012 IEEE International Conference on Computational Intelligence for Measurement Systems and Applications (CIMSA) Proceedings*, pages 7–11. IEEE, 2012.

[7] Bhavana Valeti and Shamim Pakzad. Automated detection of corrosion damage in power transmission lattice towers using image processing. In *Structures Congress 2017*, pages 474–482.

[8] S Golnaz Shahidi, Nur Sila Gulgec, and Shamim N Pakzad. Compressive sensing strategies for multiple damage detection and localization. In *Dynamics of Civil Structures, Volume 2*, pages 17–22. Springer, 2016.

[9] Nur Sila Gulgec, S Golnaz Shahidi, and Shamim N Pakzad. A comparative study of compressive sensing approaches for a structural damage diagnosis. In *Geotechnical and Structural Engineering Congress 2016*, pages 1910–1919, 2016.

[10] Yann LeCun, Yoshua Bengio, and Geoffrey Hinton. Deep learning. *Nature*, 521(7553):436–444, 2015.

[11] Yann LeCun and Yoshua Bengio. Convolutional networks for images, speech, and time-series. In *MIT Press*, 1995.

[12] Kaiming He, Xiangyu Zhang, Shaoqing Ren, and Jian Sun. Deep residual learning for image recognition. *arXiv preprint arXiv:1512.03385*, 2015.

[13] Nur Sila Gulgec, Martin Takac, and Shamim N. Pakzad. Convolutional neural network approach for robust structural damage detection and localization. *Journal of Computing in Civil Engineering*, 30(3):04015038, 2018.

[14] Nur Sila Gulgec, Martin Takáč, and Shamim N Pakzad. Structural damage detection using convolutional neural networks. In *Model Validation and Uncertainty Quantification, Volume 3*, pages 331–337. Springer, 2017.

[15] Bing Pan, Kemao Qian, Huimin Xie, and Anand Asundi. Two-dimensional digital image correlation for in-plane displacement and strain measurement: a review. *Measurement science and technology*, 20(6):062001, 2009.

[16] Satoru Yoneyama, A Kitagawa, S Iwata, K Tani, and H Kikuta. Bridge deflection measurement using digital image correlation. *Experimental Techniques*, 31(1):34–40, 2007.

[17] GOM. Aramis user manual–software, 2013.